

# Modeling of the Pile Foundation as a Nodal System with Couple Interaction

Rusakov, A.I.

It is suggested the method of numerical modeling of a pile foundation as a system of elastic links on the square nodal mesh, covering the basement surface. Each node is linked to the earth by elastic support — modeling the compression strain of a soil — and to an every adjacent node by vertical elastic link — modeling the shear strain of a soil. There derived stiffness characteristics of elastic links securing a model adequacy. There presented comparative analysis of computational results obtained by different methods.

## 1. Introduction

In practice of analysis of reinforced concrete foundations on a pile base it is widely employed finite element models (FE-MODEL) of structures where the base is specified with “button” model: either pile field (PF) is replaced by continual surface under the bottom of foundation, backing up Winkler bearing reaction, or each pile is considered as elastic support with given stiffness, with no account of bearing reaction of soil between piles. Both approaches are similar in their basis and either makes similar results. In their bounds we can not find out the increase of vertical bearing reaction under a bottom of stiff foundation on approaching to its edge [1, 2]. The seriousness of this defect is revealed by incorrect evaluation of the load to a pile at the edge of a PF and by incorrect reinforcement of the foundation slab near its edge.

In this paper we suggest the method of numerical modeling of basement as a system of elastic links on the square nodal mesh, covering the basement surface. Each node has elastic support, modeling compression strain of a soil on account of vertical nodal displacement, and the system of vertical elastic links with

adjacent nodes, modeling the shear strain of the ground. The nodal mesh of a basement is specified so that the PF-mesh would be its part. The basement nodes, situated at the pile heads, simulates the pile bearing in the FE-MODEL of the house's skeleton. The adequacy of a basement's model as a system of elastic links is attained by representation of potential energy of elastic deformation of a base soil as a function of displacements of nodes and ensuring of coincidence for this function with potential energy of elastic links' system.

## 2. The problem formalization and model parameters evaluation

Let us consider the rectangular PF with a small enough pile step  $s$  such that bearing reaction between piles is being neglectable. We suppose that the piles are absolutely rigid and their lateral dimension much lesser then the distance  $s$ . The piles are embedded into linear-deformed layer of a soil by width  $H$ , consisting of  $n$  uniform layers of a constant width  $h_i$ ,  $m$  layers of them are located below piles' ends (Fig. 1). The extension of ground body out of the PF is considered as finite but long enough; in practice for a PF of plan dimensionality  $b \times l$  it is fairly good rectangular ground body of dimensionality  $2b \times 2l \times H$ . At the basement surface we introduce the square mesh of nodes, their vertical displacements are considered to be the degrees of freedom of a basement, defining its state. Let us specify the mesh step  $s$  and choose the mesh situation such that piles' head are located at the nodes.

Let us introduce mechanical model of a basement as a system of elastic links connecting nodes in pairs and each node — with an earth (Fig. 2). If potential energy of the links ensemble being a function of nodal displacements coincides with analogous function for energy of deformation of given elastic basement, then we can affirm equivalence of mechanical model to the real basement. We imply that in this case we can obtain the stress-strain state (SSS) of the structure's skeleton as the state, corresponding to minimum of total potential energy of the system "skeleton-basement", and get it by replacement of the con-

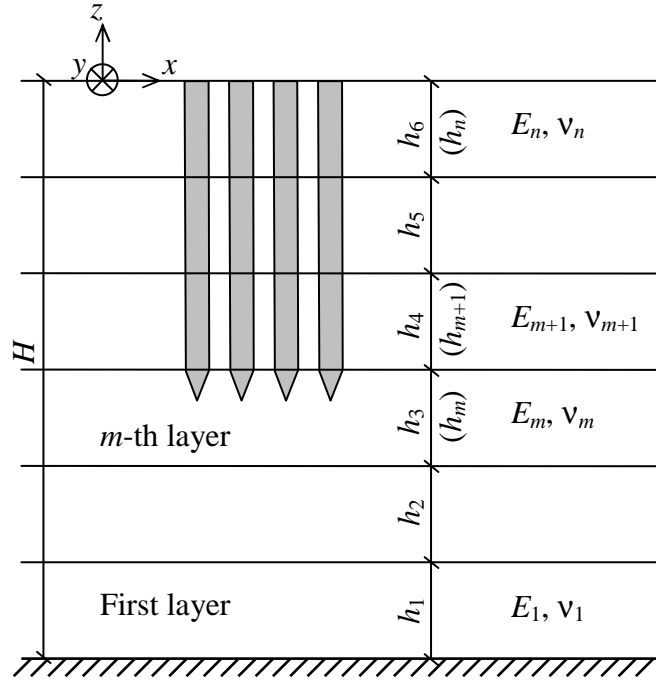


Fig. 1. The pile basement.  $E_i, \nu_i$  — deformation modulus and Poisson's ratio for  $i$ -th layer of a soil

tinuous elastic basement by its model on the “springs”. Let us find out, that approximate coincidence of potential energy of mechanical model, being a function of nodal displacements, with total deformation energy of the basement we can ensure by setting up 4 parameters — stiffness coefficients of elastic links

$$C_{1\,pile}, C_{2\,pile}, C_{1\,soil}, C_{2\,soil}. \quad (1)$$

Here index “1” points to the stiffness of the link between a node and a ground; index “2” points to the stiffness of the coupling link; index “*pile*” means that nodes with stiffness under consideration are not out of the PF; index “*soil*” means that corresponding nodes are situated on the ground outside the PF (for a coupling link no less then one node is outside the PF). In the model under consideration stiffness coefficients  $C'_2$  of coupling links on the edge of PF (Fig. 2) are calculated through stiffnesses of coupling links strictly inside and outside PF as follows:

$$C'_2 = \frac{C_{2\,pile} + C_{2\,soil}}{2}. \quad (2)$$

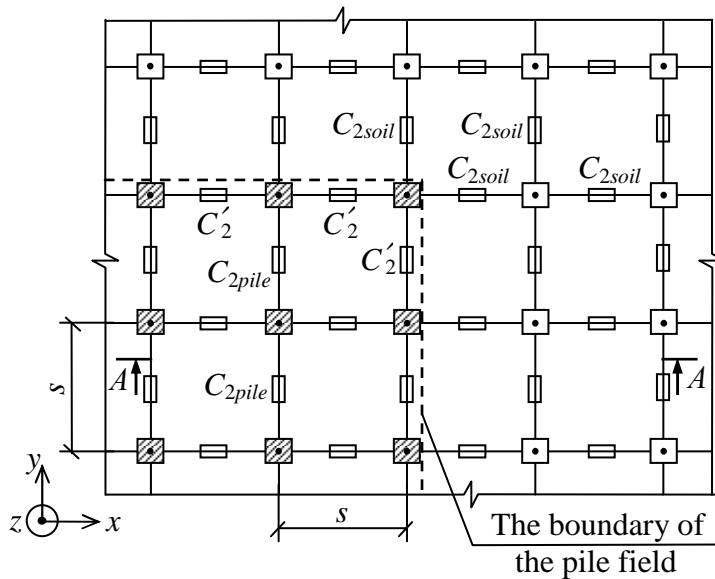


Fig. 2. Model of basement.

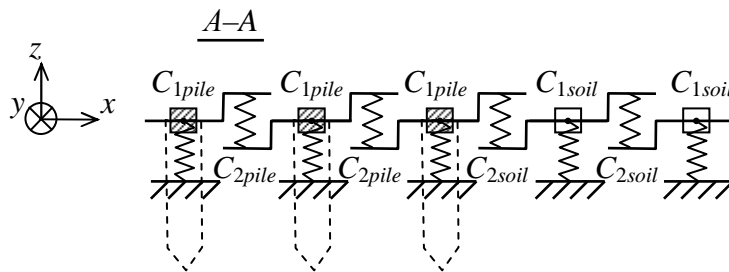
Conventions:

— — elastic link of  $z$ -direction between nodes on the grid;

▨ — node of a pile with a floating fixity;

□ — node of a soil with a floating fixity;

The link “floating fixity” cancels rotation of nodes [3]



We suppose that horizontal displacements of a soil are being zero:

$$u = v = 0. \quad (3)$$

Accordingly lateral pressure is

$$\sigma_x = \sigma_y = \frac{\nu}{1-\nu} \sigma_z. \quad (4)$$

Here and below we consider the stress in a soil induced by a loading from foundation (with no account of a soil weight).

Evaluation of the component of potential energy defined by linear deformation of a soil. Let us pick under each node a right prism of a soil, having height  $H$  and square cross-section  $s \times s$  with the node on the prism axis (Fig. 3, pos. 1). The compo-

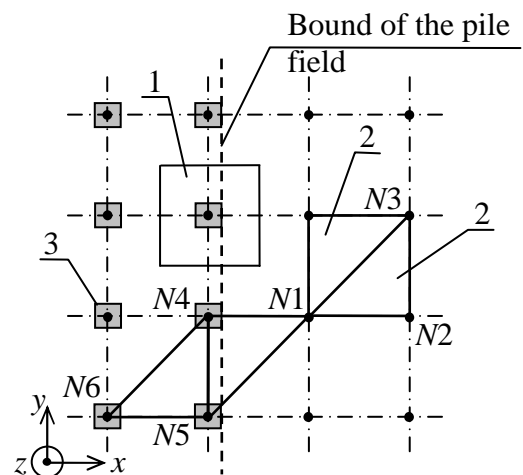


Fig. 3. Prisms in a soil's strata:

1 — quadrilateral prism;

2 — triangle prism;

3 — the pile head;

$N_i$  — the node of a basement

ment that we are after has a form [4]:

$$U_{\varepsilon pr} = \int_V U_{\varepsilon} dV; \quad U_{\varepsilon} = \frac{1}{2} \sigma_z \varepsilon_z, \quad (5)$$

where the integral is taken over a whole prism volume and we take into account that  $\varepsilon_x = \varepsilon_y = 0$ . To evaluate energy (5) we assume as follows:

1. For a prism including a pile, the stress  $\sigma_z$  under lower end of a pile is permanent along prism, whereas over the end of a pile is  $\sigma_z = 0$ .
2. For a prism not including a pile, the stress  $\sigma_z$  is permanent along prism.

Assumption 1 corresponds to Pasternak's hypotheses, specifying SSS-properties of soil's column in accordance with situation and form of its upper border surface [1]. Following by these hypotheses, in the case of plain deformed surface of a soil, the total shearing force along lateral surface of a column is null and the pressure on upper column's boundary is counteracted with the same pressure on lower boundary of linear-deformed layer. In our problem the deformed surface of conventional foundation may be considered as plain.

Assumption 2 describes SSS of a soil inadequately: as a rule, nearby the PF at the lower end of a prism the stress  $|\sigma_z|$  essentially greater then compressing stress  $\bar{\sigma}$  produced by a given shortening of prism with no shearing forces at the lateral facets, whereas this stress falls to zero on increase of  $z$ . However, by mean of assumption 2 we figure out an order of magnitude of deformation energy (5) and can establish at least rough approach of basement stiffness  $C_{1 soil}$ . This parameter we suggest to match such that mechanical model would describe best the SSS of soil deformed on Coulomb-Moor's law [5, p. 97]. The ultimate goal of mechanical model's construction is adequate description of a real soil but not its simulation as linear-elastic layer.

Let us evaluate integral (5) for a prism with a pile having a given vertical pile's node displacement  $w^u$ . After substitution (4) in generalized Hooke's law we obtain in any of  $m$  layers under lower end of a pile:

$$\varepsilon_{zi} = \psi_i \sigma_z; \quad (6)$$

$$\Psi_i \equiv \frac{1}{E_i} \frac{1 - \nu_i - 2\nu_i^2}{1 - \nu_i}. \quad (7)$$

Express  $\sigma_z$  through  $w^u$ ; for that we substitute equality (6) into expression

$$w^u = \sum_{i=1}^m \varepsilon_{zi} h_i$$

and obtain:

$$\sigma_z = \frac{w^u}{\sum_{i=1}^m \Psi_i h_i}. \quad (8)$$

Hence for bulk energy of strain of  $k$ -th layer we get:

$$U_{\varepsilon k} = \frac{1}{2} \sigma_z \varepsilon_{zk} = \frac{1}{2} \Psi_k \sigma_z^2 = \frac{1}{2} w^{u2} \frac{\Psi_k}{\left( \sum_{i=1}^m \Psi_i h_i \right)^2}.$$

For energy integral (5) we obtain:

$$U_{\varepsilon pr} = \sum_{k=1}^m U_{\varepsilon k} s^2 h_k = \frac{1}{2} s^2 w^{u2} \frac{1}{\sum_{i=1}^m \Psi_i h_i}. \quad (9)$$

For a soil prism outside the PF we can get analogous expression using assumption 2. This expression differs from (9) by the replacement of upper limit of a sum from  $m$  to  $n$ . Denote as follows:

$$C_{1pile} = \frac{s^2}{\sum_{i=1}^m \Psi_i h_i}; \quad C_{1soil} = \frac{s^2}{\sum_{i=1}^n \Psi_i h_i}. \quad (10)$$

By summarizing of energies  $U_{\varepsilon pr}$  over all prisms we obtain the total energy of linear deformation of a soil strata  $U_{\varepsilon}$  as follows:

$$2U_{\varepsilon} = \sum_{i \in \{PF\}} C_{1pile} w_i^{u2} + \sum_{i \notin \{PF\}} C_{1soil} w_i^{u2}, \quad (11)$$

where  $\{PF\}$  is a nodes' number set for nodes in the boundaries of the PF;  $w_i^u$  is a displacement of  $i$ -th node (denoted below  $Ni$ ).

Evaluation of the component of potential energy defined by shear deformation of a soil. Let us partition the compressed strata by a number of triangle right prisms such that the ribs of each one connects three adjacent nodes as it depicted on Fig. 3. Consider shear deformations that produce rotation of the rib of direction  $x$  in the plane  $xz$  by an angle  $\gamma_{xz}^u$ , and rotation of the rib of direction  $y$  in the plane  $yz$  by an angle  $\gamma_{yz}^u$ . These angles are the shear strains on the ground surface; for the prism with nodes  $N1$ — $N3$  on Fig. 3 they are depicted on Fig. 4 and are represented through vertical displacements  $w_i^u$  of corresponding nodes  $Ni$  as follows:

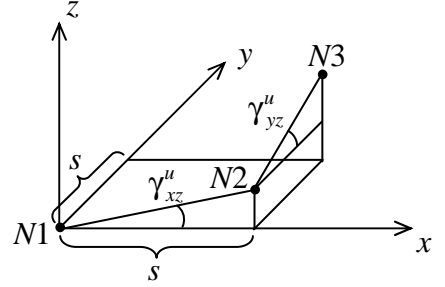


Fig. 4. Nodal displacements in the shear case

$$\gamma_{xz}^u = \frac{w_2^u - w_1^u}{s}; \quad \gamma_{yz}^u = \frac{w_3^u - w_2^u}{s}. \quad (12)$$

For any other prism these formulas are also being correct (neglecting the sign of a shear angle) for convenient enumeration of nodal displacements. The component of deformation energy caused by shear has the next form for triangle prism:

$$U_{\gamma pr} = \int_V U_{\gamma} dV; \quad U_{\gamma} = \frac{1}{2}(\tau_{xz} \gamma_{xz} + \tau_{yz} \gamma_{yz}) = \frac{1}{2} G_k (\gamma_{xz}^2 + \gamma_{yz}^2), \quad (13)$$

in account of  $\gamma_{xy} = 0$ . Here  $G_k = \frac{E_k}{2(1 + \nu_k)}$  is shear modulus of  $k$ -th layer.

For evaluation of energy (13) we add next assumptions to the late ones:

3. The shear strain is constant in a horizontal section of triangular prism.
4. The shear strain distribution diagram over the altitude is proportional to diagram for vertical displacements of a soil, which accords to assumptions 1—2.

The validity of assumption 3 is secured by a small enough step  $s$  of the PF mesh. Assumption 4 is a consequence of Pasternak's hypotheses about the SSS

of a soil's column with plain upper border surface [1, p. 52]: the distribution diagrams of vertical displacements  $w_I$  and  $w_{II}$  on two verticals inside that column are proportional, hence diagram for difference  $w_I - w_{II}$  is also proportional, but the latter is a diagram of a shear angle (by accuracy to coefficient).

At first, let us consider a prism having at least one node out of the PF. The diagram of displacements  $w$  on a vertical basic line inside such prism is monotonous piecewise-linear (Fig. 5, on the left). The ordinates at the bounds of layers may be evaluated by substitutions (6) and (8) after replacement  $m$  by  $n$ :

$$w_j = \sum_{i=1}^j \varepsilon_{zi} h_i = q_j w^u, \quad j = \overline{0, n};$$

$$q_j \equiv \frac{\sum_{i=1}^j \psi_i h_i}{\sum_{i=1}^n \psi_i h_i} \quad \text{for } j = \overline{1, n}; \quad q_0 \equiv 0. \quad (14)$$

On Fig. 5 it is depicted proportional diagram of the shear angle for which there holds:

$$\gamma_j = q_j \gamma^u, \quad j = \overline{0, n}. \quad (15)$$

Let us evaluate the energy of shear deformation for a part of a prism situated at  $k$ -th layer of a soil. Translate an origin of coordinate  $z$  to the bottom of  $k$ -th layer. We have:

$$U_{\gamma^k} = \frac{s^2}{2} \int_0^{h_k} \frac{1}{2} G_k (\gamma_{xz}^2 + \gamma_{yz}^2) dz, \quad (16)$$

where for each strain  $\gamma_{xz}$ ,  $\gamma_{yz}$  it holds:

$$\gamma = \gamma_{k-1} + \frac{\gamma_k - \gamma_{k-1}}{h_k} z. \quad (17)$$

After substitutions (15) into (17) and (17) into (16) we obtain:

$$U_{\gamma^k} = \frac{s^2}{4} G_k \frac{h_k}{3} (q_{k-1}^2 + q_{k-1} q_k + q_k^2) (\gamma_{xz}^{u^2} + \gamma_{yz}^{u^2}). \quad (18)$$



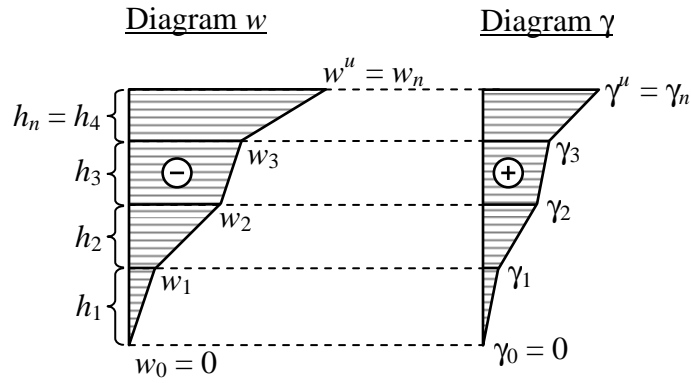


Fig. 5. Soil strain diagrams outside the PF  
(case  $n = 4$ )

Set value as follows:

$$C_2 = \frac{1}{3} \sum_{k=1}^n G_k h_k (q_{k-1}^2 + q_{k-1} q_k + q_k^2). \quad (19)$$

After substitutions (12) in formula (18) and summation by  $k$  we obtain search energy (13) as follows:

$$U_{\gamma pr} = \frac{1}{2} \frac{C_2}{2} \left[ (w_2^u - w_1^u)^2 + (w_3^u - w_2^u)^2 \right]. \quad (20)$$

For triangular prism inside the PF formulas (19), (20) are being correct if we alter formula (14) as follows:

$$q_j = \frac{\sum_{i=1}^j \psi_i h_i}{\sum_{i=1}^m \psi_i h_i} \text{ for } j = \overline{1, m}; \quad q_0 = 0; \quad q_j = 1 \text{ for } j = \overline{m+1, n}. \quad (21)$$

This demand ensues out of affirmation that shear angle in the inter-piles' bulk is constant by height, just like the soil displacement on the vertical basic line.

On summarization of shear energy over all prisms the addends with expression  $(w_i^B - w_j^B)^2$  is augmented twice, because every rib, connecting nodes  $N_i$  and  $N_j$ , belongs to two adjacent prisms<sup>1</sup>. Let us denote

<sup>1</sup> For prisms at a border of a soil bulk it's not right, but on the remote distance from the PF the properties of a soil are not significant for SSS of a mat. Corresponding error of energy calculation is neglected.

$$C_{2soil} = C_2 \text{ after substitutions (14); } C_{2pile} = C_2 \text{ after substitutions (21).} \quad (22)$$

Then total shear strain energy of a soil strata  $U_\gamma$  may be written as follows:

$$2U_\gamma = \sum_{i,j \text{ inside PF}} C_{2pile} (w_i^u - w_j^u)^2 + \sum_{i,j \text{ outside PF}} C_{2soil} (w_i^u - w_j^u)^2 + \sum_{i,j \text{ over edge of PF}} C_2' (w_i^u - w_j^u)^2. \quad (23)$$

Here  $C_2'$  is defined by formula (2); summation is over all pairs  $(i, j)$  such that a distance between nodes  $N_i$  and  $N_j$  is equal to  $s$ , moreover the first sum includes all pairs of nodes inside the PF (but not on its border), second sum includes all pairs for which at least one node is outside the PF, third sum includes all pairs, located at the contour of the PF. In the example on Fig. 3 pair (5, 6) belongs to the first sum, pair (4, 1) to the second sum, and pair (4, 5) to the third sum.

The total potential deformation energy of soil strata, evaluated by summarization of expressions (11) and (23) taken with coefficient  $\frac{1}{2}$ , is a function of displacements  $w_i^u$ , that coincides to analogous function for potential energy of elastic links of 4-parametrical mechanical model on Fig. 2. The coincidence of functions for potential energy of a model and soil strata signifies equivalence of a model to the ground under consideration as a system of finite degrees of freedom.

The method of a pile basis simulation by means of the system of elastic links with parameters defined by formulas (10) and (22) we nominate the method of elastic links.

### 3. Method approbation

An adequacy of methods of analysis of a foundation's mat with pile basis has been checked for any typical foundations. For each of them it has been compared numerical results of analysis by the model with elastic links, by the linear-elastic FE-model of a base, and by FE-model with Mises-Schleicher condition of marginal state of a soil [6, p. 76] (Coulomb's soil).

For analysis of pile loading we consider the example of stiff square mat 19,5×19,5 m, loaded under pressure 25 ton/m<sup>2</sup> (this average characteristic pressure on a base is produced by a foundation of 17-storage house with complete skeleton). The PF below the mat has a grid of 1.5 m step; the number of soil layers under the mat is  $n = 3$ ,  $m = 2$ ; their characteristics are represented by Table 1.

Table 1

$i$	Soil kind	$h_i$ , M	$E_i$ , ton/m <sup>2</sup>	$\nu_i$	$\varphi_i$ , degree	$c_i$ , ton/m <sup>2</sup>
1	sand	4	2000	0,3	30	0,5
2	clay	6	1000	0,35	13	3
3	clay	10	1000	0,35	13	3

The comment.  $\varphi_i$  — the angle of internal friction;  $c_i$  — cohesion coefficient.

On Fig. 6 it is depicted the first quadrant of the PF with distribution diagrams of pile loading along two basic lines<sup>2</sup>. The pile's load calculated by means of "button" model is the constant value  $N_{but} = 49$  ton. For considered design model this number defines demanded working load on the pile in analysis with button model. The strength capacity of a pile is obtained by scaling the working load with reliability coefficient and may reach about 70 ton. This is much lower

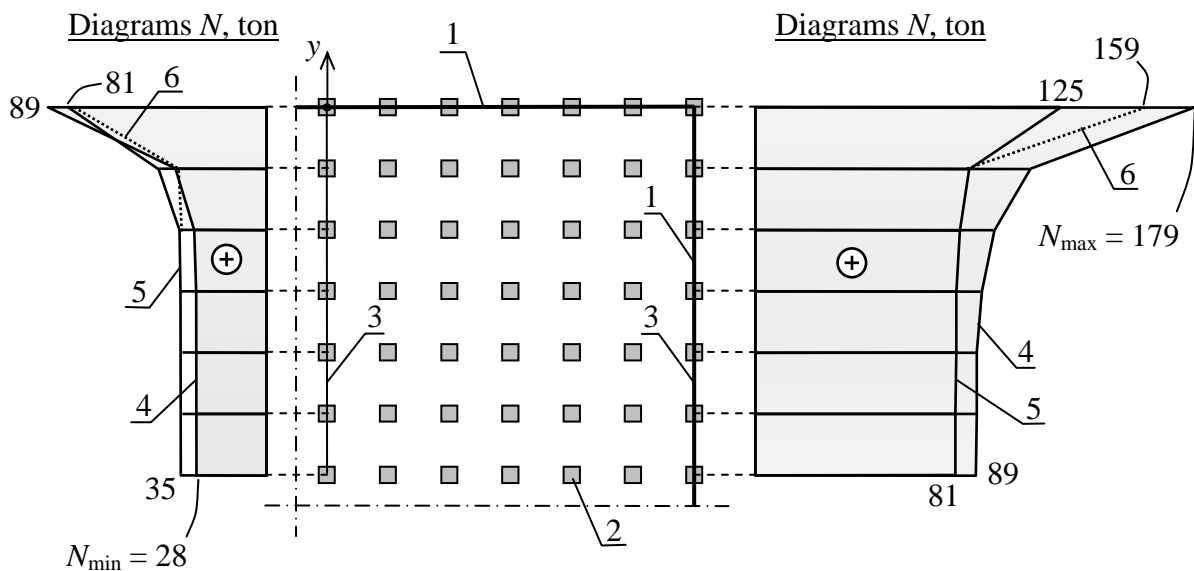


Fig. 6. The diagrams of vertical pressing loads on the pile heads. 1 — outline of the mat in the design model; 2 — pile heads; 3 — diagram's basic line; 4 — diagram for linear-elastic soil; 5 — diagram for Coulomb's soil; 6 — diagram for the model of soil as the system of elastic links

<sup>2</sup> Only the ordinates of diagrams situated opposite corresponding piles makes the physical sense.

then load 125 ton applied to corner's pile in Coulomb's soil case and any lower than load 81 ton on a pile in the middle of outer row (Fig. 6, diagram pos. 5). That is why in the case of button model analysis we have to expect the overtolerance load for the piles at an edge of the PF. The calculations point out also, that linear-elastic model distorts the pile load distribution producing its nonuniformity: the load ratio  $N_{\max}/N_{\min}$  is 6.4 for this model, whereas by the most reliable nonlinear calculations this ratio is equal to 3.6.

The simulation of the pile basement by the method of elastic links results in distribution of pile loads depicted with dashed diagram, pos. 6, on Fig. 6. The loads on the most of piles happened to be so close to the results of nonlinear analysis that diagrams, pos. 5 and 6, coincide at the significant extent. The load on the corner pile by the new method is  $N_{\max} = 159$  ton, that is medium value between results of computing by means of linear and nonlinear models. We have to remark that observed accuracy of calculation of pile loads through the method of elastic links is obtained with the model, in which parameter  $C_{1\ soil}$  wasn't optimized but has been specified by assumption 2.

It is adequately described by the new method the shape and depth of settling impression. For the example considered above the settlement caused by additional pressure under the conventional foundation occurred to be equal: in linear-deformed layer scheme — 76 mm; in the FEM-analysis with Coulomb's law usage — 78 mm; in the method of elastic links — 79 mm. On Fig. 7 it is depicted diagrams of vertical displacement of ground surface along  $y$ -axis (Fig. 6). Zero abscissa corresponds to marginal pile at this axis. Relation 1 is the case of Coulomb's soil; relation 2 is the case of ground's model as a system of elastic links. It may be seen that difference of corresponding displacements near the mat is neglectable.

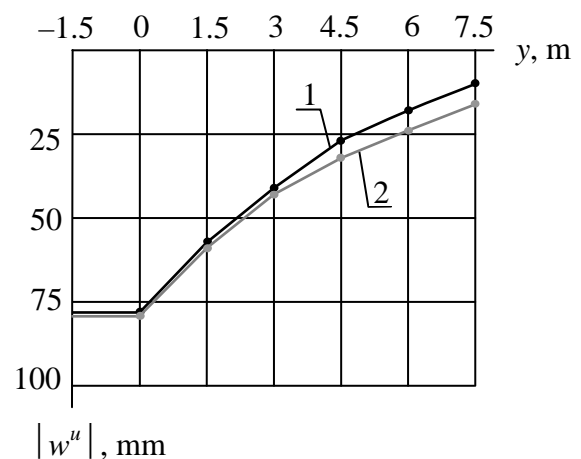


Fig. 7

The efficiency of SSS-analysis of monolithic floor through the method of elastic links is tested on several models. For instance, it was considered the FE-model of 14-storey house with stiff load-bearing walls over perimeter of foundation mat, and 4 columns inside mat's plan (Fig. 8, *a*). The mat is of width of 1.2

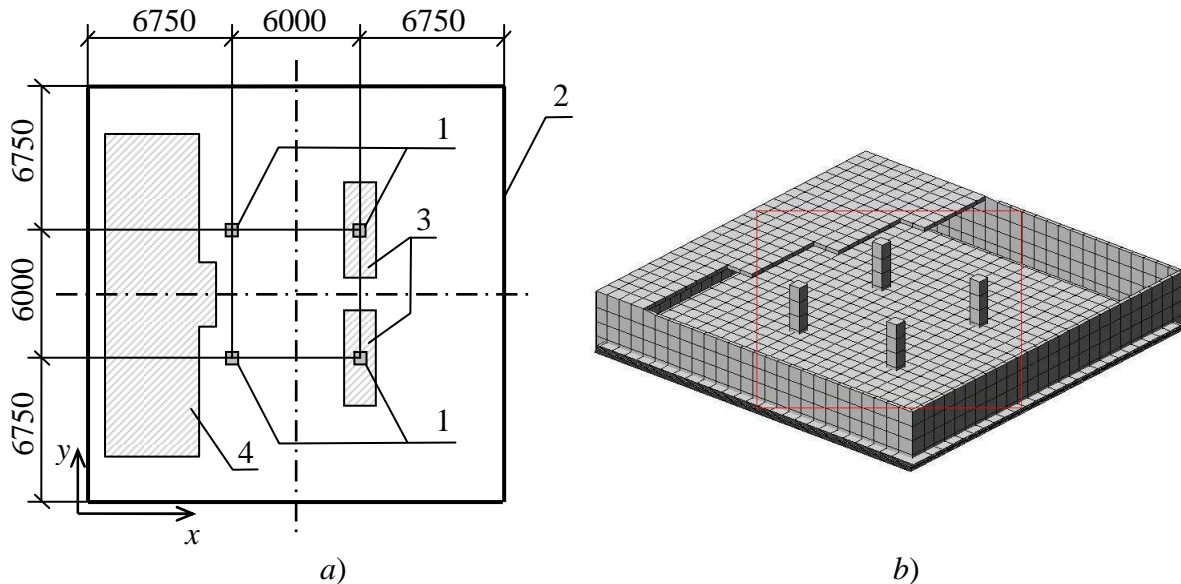


Fig. 8. Test model of mat reinforcement: *a*) plan of constructions on the mat; *b*) design model in graphics of PP LIRA (floor shown partially). 1 — column; 2 — walling; 3 — region of additional lower reinforcement of  $x$ -direction; 4 — region of additional upper reinforcement of  $x$ -direction. Distance dimension is mm

m has been built on the basement described above (Fig. 6). Symmetry axes shown on Fig. 6 defines as well symmetry plains of house structure. The design model includes first storey constructions and a floor above (Fig. 8, *b*). Constructions over this floor are specified by equivalent loading distributed over the floor, and proper choice of weight for walls and columns. Total design loading applied to constructions, shared to mat area, is of  $24.1 \text{ ton/m}^2$ .

The design model on Fig. 8, *b*, has been used to compare the mat reinforcement by means of next FE-models: model A with the basement of button model type; model B for which the basement is modeled as a system of solid FE of a soil deformed under Coulomb's law; model C with the basement specified by elastic links method; model D for which the basement is modeled with FEM as elastic layer. For each model we established the range of longitudinal reinforcement area at the regions of additional reinforcement. The region of addi-

tional lower reinforcement has been set with model B, the region of additional upper reinforcement has been set with model A. Let us denote the design intensity of reinforcement, accordingly, for lower one by  $A_l$ , for upper one by  $A_u$ . Demanded areas of reinforcement at noted regions (Fig. 8, *a*) are tabulated in Table 2. The conditions of analysis: concrete B25, reinforcement A-III, the crack opening is being accounted.

Table 2

Model	$A_l$ , cm <sup>2</sup> /m	$A_u$ , cm <sup>2</sup> /m
A	6÷12	14÷33
B	14÷38	6÷20
C	17÷39	6÷17
D	31÷52	6÷15

One can see, that taking into account the Coulomb's slip for soil layers (case B) causes essential increase of lower reinforcement area comparatively to button model. At the same time button model makes excessive demands to upper reinforcement at exterior panel. The results of reinforcement most close to case B are obtained by means of the model with elastic links. FEM-analysis with elastic solid elements resulted in excessive increase of lower reinforcement area under the columns and excessive decrease of upper reinforcement area at the middle of panels.

FE-submodel of basement with account of Coulomb's slip is not always applied because of its great demands to computer resources. In particular, the run-time may exceed 10 hours for processor of 2—3 GHz. At the same time the method of elastic links for basement simulation uses practically the same resources as the button model.

In the fulfilled testing calculation by the method of elastic links it wasn't necessary to optimize parameter  $C_{1soil}$  through matching the results by this method and by FEM with nonlinear submodel of soil deformations, because the results obtained with these methods turned out initially close. But for definite soil conditions the correction of  $C_{1soil}$  might be necessary. In this case usage of simplified FE-models with account of Coulomb's slip will be enough.

### Results.

Modeling of a pile basement through new method of elastic links suggests representation of basement as a system of nodes, connected by elastic links to an

earth and to each other node in pairs. By numerical results of pile loads, settlements and reinforcement of a mat, the method makes good correspondence to nonlinear FE-model with account of Coulomb's deformation of a soil. At the same time the new method demands insignificant computer resources for SSS analysis.

The method of pile basement simulation with elastic solid FE of a soil makes essential distortions in design reinforcement of a mat because it raises loads on marginal piles and diminishes loads on piles inside slab's plan. The distortion is evinced by augmentation of lower reinforcement area under columns at the exterior panels and by diminishing of upper reinforcement in the middle of the same panels.

The method of analysis of pile basis by means of button model gives inadequate results of mat reinforcement. The calculations through this method result in diminishment of lower reinforcement area under columns at the exterior panels and in augmentation of upper reinforcement in the middle of the same panels. Pile loads, obtained with this method, are diminished at the verge of foundation mat and augmented inside the plan of a mat.

## REFERENCES

1. Pasternak, P.L., The basics of a new method for analysis of foundations on elastic basement by means of two modules of subgrade reaction. Moscow, Stroiizdat, 1954, 56 p. (in Russian)
2. Sozanovitch, M.E., About some aspects of foundation analysis. Industrial and Civil Engineering, 2006, No. 8, pp. 60–61. (in Russian)
3. Rusakov, A.I., Structural mechanics. (Stroitel'naya mehanika.) Moscow, "Prospekt", 2004. 360 p. (in Russian)
4. Rusakov, A.I., Course of Lectures on Strength of Materials. Rostov-on-Don, "Kniga", 2004, 326 p. (in Russian)

5. Vyalov, S.S., Rheological Principles of Soil Mechanics. Moscow, Higher School Publishing House, 1978, 447 p.
6. Strelets-Streletski, E.B., and others, LIRA 9.2. User Manual. Basics. The textbook. Edited by Gorodetski A.S., Kiev, Fact, 2005, 145 p. (in Russian)